Research Paper

New Surface-Plasmon-Polariton-Like Acoustic Surface Waves at the Interface Between Two Semi-Infinite Media

Piotr KIEŁCZYŃSKI

Institute of Fundamental Technological Research, Polish Academy of Sciences
Warsaw, Poland; e-mail: pkielczy@ippt.pan.pl

This paper presents theory of new shear horizontal (SH) acoustic surface waves that propagate along the interface of two semi-infinite elastic half-spaces, one of which is a conventional elastic medium and a second one an elastic metamaterial with a negative and frequency dependent shear elastic compliance.

This new surface waves have only one transverse component of mechanical displacement, which has a maximum at the interface and decays exponentially with distance from the interface. Similar features are also shown by the acoustic shear horizontal Maerfeld-Tournois surface waves propagating at the interface of two semi-infinite elastic media due to the piezoelectric effect that should occur in at least one semi-space.

The proposed new shear horizontal acoustic surface waves exhibit also strong formal similarities with the electromagnetic surface waves of the surface plasmon polariton (SPP) type, propagating along a metal-dielectric planar interface. In fact, the new shear horizontal elastic surface waves possess a large number of properties that are inherent for the SPP electromagnetic surface waves, such as strong subwavelength concentration of the wave field in the proximity of the guiding interface, low phase and group velocity etc. As a result, the new shear horizontal acoustic surface waves can find applications in sensors with extremely high sensitivity, employed in measurements of various physical parameters, such as viscosity of liquids, as well as in biosensors, chemosensors, or a near field acoustic microscopy (subwavelength imaging) and miniaturized devices of microwave acoustics.

Keywords: shear horizontal acoustic waves; surface plasmon polaritons; phase velocity; group velocity; Poynting vector.

1. Introduction

Acoustic surface waves typically exist on the free surface of solid media or at the interface between two different elastic materials. The mechanical displacement of these surface waves should decrease exponentially as we move away from the surface (interface) into the bulk of solid materials. Acoustic surface waves occur in nature, e.g. Rayleigh, Love, Stoneley waves (ACHENBACH, 1973; AULD, 1990; ROYER, DIEULESAINT, 2000).

Surface waves have found application in many fields of technology such as: 1) seismology (Rayleigh, Love, Stoneley, Sezawa waves) and 2) electronics (Rayleigh waves – filters in cellular telephony, Love waves in sensors of physical quantities, e.g. viscosity of liquids, in biosensors and chemosensors).

Shear horizontal (SH) acoustic surface waves, with one transverse component of mechanical vibrations, form a special class of elastic surface waves due to their inherent affinities and connections to electromagnetic surface waves and quantum mechanical systems. For example, shear horizontal surface waves of the Love type (LOVE, 1911), which propagate in layered planar elastic waveguides, are analogous to transverse magnetic (TM) electromagnetic modes in metalized dielectric waveguides of integrated optics and to quantum particles in a rectangular potential well (KIEŁCZYŃSKI, 2021). This is due to the fact that these three different physical phenomena are described by a common mathematical model, i.e. the direct Sturm-Liouville problem.

Among the surface waves, a special role is played by the class of acoustic surface shear horizontal (SH) waves, such as the Love, Bleustein–Gulyaev and Maerfeld–Tournois waves (ROYER, DIEULESAINT, 2000). Love waves are shear horizontal waves propagating in layered waveguides composed of surface elastic

layer deposited on an elastic substrate (Love, 1911). Bleustein-Gulyaev waves are also shear horizontal surface acoustic waves that propagate on the surface of piezoelectric half-spaces with appropriate symmetry (Bleustein, 1968). Another example of shear horizontal waves are Maerfeld–Tournois waves, which propagate along the interface of two elastic half spaces, at least one of which is a piezoelectric medium with an appropriately directed symmetry axis (Maerfeld, Tournois, 1971).

It can be proved that shear horizontal surface acoustic wave cannot exist on the surface of a purely elastic half-space (Achenbach, 1973). Similarly, it can also be shown that shear horizontal surface wave cannot propagate at the interface of two elastic half-spaces, regardless of their symmetry and/or orientation.

In this paper we will challenge this assertion, showing that the SH elastic surface waves can propagate along at the interface between two elastic-half-spaces, providing that one of them is an elastic metamaterial with special properties, i.e. with a negative shear elastic compliance $s_{44}^{(1)}$ (see Eq. (1)). Moreover, in contrary to shear horizontal acoustic interfacial waves of the Maerfeld–Tournois type, the proposed new shear horizontal acoustic surface waves can exist in waveguides that are entirely devoid of the piezoelectric effect. The mechanical displacement of this new wave diminishes exponentially as it moves away from the interface surface. Hence, this new acoustic wave is an evanescent type wave in the direction perpendicular to the interface.

Acoustic waves in metamaterials were the subject of the several works (Deng *et al.*, 2014; Ambati *et al.*, 2007; Kadic *et al.*, 2013; Zaccherini *et at.*, 2020; Yu *et al.*, 2020). However, these papers concerned other types of waves, i.e. Rayleigh waves on the solid-vacuum interface (Deng *et al.*, 2014), Scholte waves on the solid-liquid interface (Deng *et al.*, 2014), bulk waves (Ambati *et al.*, 2007; Kadic *et al.*, 2013; Zaccherini *et at.*, 2020), but not shear acoustic surface waves, which are considered in this paper.

In this paper, the author presents a mathematical model describing the properties of a new SH acoustic surface wave. The dispersion equation of this new elastic surface wave, the mechanical displacement u_3 distributions and the dispersion curves of this new wave were determined. The fundamental properties of the proposed surface wave are presented. Possible practical applications of this new surface wave are also given.

It is worth noting that this new acoustic surface wave is a direct analog of SPP electromagnetic wave propagating along the metal-dielectric interface (Zhang *et al.*, 2012; Maier, 2007). The equivalent of the transverse mechanical displacement u_3 in the new proposed acoustic surface wave is the TM field H_3 of the surface electromagnetic wave of the SPP type.

The new acoustic surface waves inherit a large number properties of the electromagnetic surface waves of the SPP type. Among others, new acoustic surface waves are characterized by a strong subwavelength concentration of the wave field in the proximity of the interface.

The dispersion curves of the new wave are also presented, i.e. graphs of the dependence of the circular frequency ω on the propagation constant K of the wave, as well as plots of the mechanical displacement distribution u_3 of the wave as a function of the distance from the interface ($x_2 = 0$) along the x_2 axis.

The analytical expression for the group velocity of the wave has been developed. This expression allows us to plot the relation of the group velocity versus frequency. It is worth noting that the group velocity as well as the phase velocity tend to zero when the wave frequency f approaches the surface resonant frequency f_{sp}.

A similar tendency is also observed for the total power transmitted by the surface wave. The total power transferred by the surface wave also converges to zero when the wave frequency $f \to f_{sp}$.

Due to a high concentration of the energy near the guiding interface $x_2 = 0$, the new SH acoustic (ultrasonic) surface waves can be used in extremely high sensitivity physical sensors, in biosensors and chemosensors. Similarly, due to the high level of the subwavelength confinement, the new SH acoustic surface waves can be used in a subwavelength near field acoustic microscopy as well as in miniaturized micro and nanoscale modern acoustic devices.

2. Mathematical model of the wave. The direct Sturm-Liouville problem

The propagation of the acoustic (ultrasonic) surface waves along the planar interface between two elastic semi-spaces, given their material parameters, can be formulated in terms of the direct Sturm–Liouville problem (Kiełczyński *et al.*, 2015; Kiełczyński, 2018). A solution to this direct Sturm–Liouville problem is in a form of discrete eigenvalue-eigenvector pairs $(K, u_3(x_2))$. An eigenvalue K is the wave number (i.e. it determines the phase velocity $v_p = \omega/K$) of the surface wave and the corresponding eigenvector $u_3(x_2)$ is a function describing distribution of the mechanical displacement u_3 of the elastic surface wave as a function of the distance from the guiding interface ($x_2 = 0$).

2.1. Geometry and material parameters of the waveguide

The waveguide supporting new SH acoustic (ultrasonic) surface waves consists of two semi-infinite elastic half-spaces, one of which is a conventional elastic material ($x_2 \geq 0$) and the second an elastic metamaterial

$(x_2 < 0)$ with a negative elastic compliance $s_{44}^{(1)}(\omega) < 0$ that is a function of angular frequency ω. By contrast, the densities $(\rho_1, \rho_2) > 0$ in both half-spaces and the elastic compliance $s_{44}^{(2)} > 0$ are positive and frequency independent (Fig. 1).
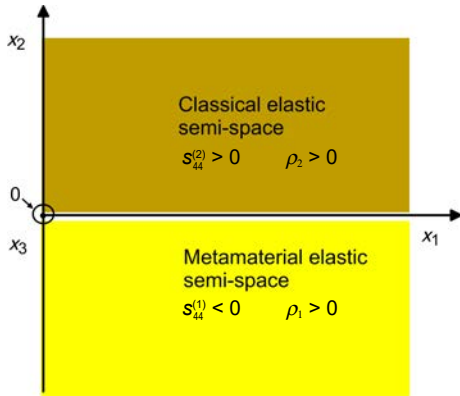

Fig. 1. Cross-section of the proposed surface wave waveguide supporting new acoustic surface waves, propagating in the direction x_1, with the mechanical displacement $u_3(x_2)$ polarized along the x_3 axis and decaying exponentially in the transverse direction x_2. Conventional elastic half-space $(x_2 \geq 0)$ and metamaterial elastic half-space $(x_2 < 0)$ are rigidly bonded at the interface $x_2 = 0$.

The proposed new shear acoustic surface wave has only one transverse component of the mechanical displacement u_3 that is polarized along the axis x_3 and parallel to the guiding interface $(x_2 = 0)$. Since polarization of the new wave is perpendicular to the direction of propagation x_1 (Fig. 1), the new shear horizontal elastic surface wave is of the transverse type.

2.1.1. Elastic parameters of the lower metamaterial semi-space

The key assumption made in this paper is about the elastic compliance $s_{44}^{(1)}(\omega)$ in the metamaterial half-space $(x_2 < 0)$. Namely, it is assumed throughout this paper that $s_{44}^{(1)}(\omega)$ in the metamaterial half-space $(x_2 < 0)$, as a function of angular frequency ω, is given by the following formula (Wu *et al.*, 2011):

$$s_{44}^{(1)}(\omega) = s_0 \cdot \left(1 - \frac{\omega_p^2}{\omega^2}\right), \qquad (1)$$

where s_0 is the elastic shear compliance of the homogeneous background material, ω_p is an angular frequency of local mechanical resonances of the microresonators embedded into the bulk of the homogeneous material of the lower half-space.

It has to be noted that the elastic compliance $s_{44}^{(1)}(\omega)$ of the metamaterial half-space $(x_2 < 0)$ is described by formally the same formula as the dielectric function $\varepsilon(\omega)$ in Drude's model of metals (Born, Wolf, 1980).

In the case of elastic metamaterials, the elastic compliance s_{44} corresponds to the dielectric constant ε for dielectric and metallic materials. Similarly, the density ρ of elastic metamaterials corresponds to the magnetic permeability μ of dielectric and metallic materials, respectively.

For $\omega < \omega_p$, the elastic compliance $s_{44}^{(1)}$ of the lower half-space takes negative values $s_{44}^{(1)} < 0$. It is worth noticing that the elastic compliance of the upper half-space is always real and positive $s_{44}^{(2)} > 0$. In the waveguide structures of this type, a SH surface acoustic wave can occur, provided that the constituent compliances satisfy the conditions given in Eq. (18).

In this study, the local bulk oscillators frequency $f_p = \omega_p/2\pi$ was assumed to be $f_p = 1$ MHz. Consequently, the surface resonant frequency f_{sp} in this metamaterial half-space equals

$$f_{sp} = \frac{f_p}{\sqrt{\left(1 + s_{44}^{(2)}\Big/s_0\right)}} = 143.569 \text{ kHz}.$$

2.2. Governing differential equations

The mechanical displacement u_3 of an acoustic surface wave must satisfy in both (upper and lower) half-spaces, the equations of motion resulting from Newton's laws of dynamics.

2.2.1. Lower metamaterial elastic half-space $(x_2 < 0)$

The mechanical displacement $u_3^{(1)}$ of the surface wave in the lower metamaterial elastic half space satisfies the following equation of motion:

$$\frac{1}{v_1^2}\frac{\partial^2 u_3^{(1)}}{\partial t^2} = \frac{\partial^2 u_3^{(1)}}{\partial x_1^2} + \frac{\partial^2 u_3^{(1)}}{\partial x_2^2}, \qquad (2)$$

where $v_1 = \left(1/(s_{44}^{(1)}\rho_1)\right)^{1/2}$ is the bulk shear wave velocity in the lossless metamaterial medium, $s_{44}^{(1)}$ is its elastic compliance, and ρ_1 is the density.

2.2.2. Upper isotropic elastic half-space $(x_2 > 0)$

The mechanical displacement $u_3^{(2)}$ of the surface wave in the elastic upper half-space satisfies the following partial differential equation:

$$\frac{1}{v_2^2}\frac{\partial^2 u_3^{(2)}}{\partial t^2} = \frac{\partial^2 u_3^{(2)}}{\partial x_1^2} + \frac{\partial^2 u_3^{(2)}}{\partial x_2^2}, \qquad (3)$$

where $v_2 = \left(1/(s_{44}^{(2)}\rho_2)\right)^{1/2}$ is the velocity of the bulk shear wave in the elastic upper half-space, $s_{44}^{(2)}$ is its elastic compliance, and ρ_2 is the density. Since $s_{44}^{(2)}$ and ρ_2 are real, the phase velocity v_2 is a real quantity as well.

2.3. Mechanical displacement and shear stresses of the surface wave

It is assumed that the new SH acoustic surface waves, propagating in waveguides depicted in Fig. 1, are time-harmonic ($\exp(-j\omega t)$), propagate in the direction of axis x_1 ($\exp(jKx_1)$), and are uniform along the transverse axis x_3.

The mechanical field of the acoustic surface wave should be concentrated in the vicinity of the interface between the two media ($x_2 = 0$). Therefore, the mechanical displacement and shear stresses of the acoustic wave should decrease exponentially as it moves away from the interface, namely:

1) in the lower metamaterial elastic half-space ($x_2 < 0$):

$$u_3^{(1)}(x_1, x_2, t) = A \cdot \exp(q_1 x_2) \cdot \exp[j(Kx_1 - \omega t)], \quad (4)$$

$$
\begin{aligned}
\tau_{13}^{(1)} &= \frac{1}{s_{44}^{(1)}} \frac{\partial u_3^{(1)}}{\partial x_1} \\
&= \frac{1}{s_{44}^{(1)}} A \cdot jK \cdot \exp(q_1 x_2) \cdot \exp[j(Kx_1 - \omega t)], \quad (5)
\end{aligned}
$$

$$
\begin{aligned}
\tau_{23}^{(1)} &= \frac{1}{s_{44}^{(1)}} \frac{\partial u_3^{(1)}}{\partial x_2} \\
&= \frac{1}{s_{44}^{(1)}} A \cdot q_1 \cdot \exp(q_1 x_2) \cdot \exp[j(Kx_1 - \omega t)]; \quad (6)
\end{aligned}
$$

2) in the upper isotropic elastic half-space ($x_2 > 0$):

$$u_3^{(2)}(x_1, x_2) = B \cdot \exp(-q_2 x_2) \cdot \exp[j(Kx_1 - \omega t)], \quad (7)$$

$$\tau_{13}^{(2)} = \frac{1}{s_{44}^{(2)}} \frac{\partial u_3^{(2)}}{\partial x_1} = \frac{1}{s_{44}^{(2)}} B \cdot jK \cdot \exp[j(Kx_1 - \omega t)], \quad (8)$$

$$
\begin{aligned}
\tau_{23}^{(2)} &= \frac{1}{s_{44}^{(2)}} \frac{\partial u_3^{(2)}}{\partial x_2} = \frac{1}{s_{44}^{(2)}} B \cdot (-q_2) \\
&\quad \cdot \exp(-q_2 x_2) \cdot \exp[j(Kx_1 - \omega t)], \quad (9)
\end{aligned}
$$

where q_1 and q_2 are the transverse wavenumbers of the elastic surface wave, K is the wave number of a new mechanical surface wave which determines the phase velocity $v_p = \omega/K$, the angular frequency is denoted by ω, A, and B are constants.

Formulas for shear stresses will be used in the boundary conditions and the component of the Poynting vector P_1 (Eqs (21) and (22)).

Introducing Eq. (4) into Eq. (2) and Eq. (7) into Eq. (3), we get:

$$q_1^2 = K^2 - k_1^2, \quad (10)$$

$$q_2^2 = K^2 - k_2^2, \quad (11)$$

where $k_1^2 = \omega^2 \rho_1 s_{44}^{(1)}$ and $k_2^2 = \omega^2 \rho_2 s_{44}^{(2)}$.

In order to provide an exponential decay of the amplitude of the new shear horizontal elastic surface wave, the transverse wavenumbers q_1, q_2 have to be real and positive.

2.4. Boundary conditions

On the interface ($x_2 = 0$) of two half-spaces, the continuity of the mechanical displacement u_3 and shear stress τ_{23}, should be provided, namely:

$$u_3^{(1)}\big|_{x_2=0} = u_3^{(2)}\big|_{x_2=0}, \quad (12)$$

$$\tau_{23}^{(1)}\big|_{x_2=0} = \tau_{23}^{(2)}\big|_{x_2=0}. \quad (13)$$

2.5. Dispersion equation of the surface wave

The boundary conditions imply that the components of the mechanical displacement u_3 and shear stress τ_{23} at the interface ($x_2 = 0$) should be continuous.

After substituting Eqs (4) and (7) to the boundary conditions Eqs (12) and (13), we obtain a system of two linear and homogeneous equations for the coefficients A and B:

$$A - B = 0, \quad (14)$$

$$\frac{q_1}{s_{44}^{(1)}} A + \frac{q_2}{s_{44}^{(2)}} B = 0. \quad (15)$$

For a nontrivial solution, the determinant of this set of linear algebraic equations for A and B must equal zero (necessary condition). Consequently, from Eqs (14) and (15), we get the following dispersion equation for the new elastic surface wave propagating along the interface ($x_2 = 0$):

$$\frac{q_2}{s_{44}^{(2)}} = -\frac{q_1}{s_{44}^{(1)}}. \quad (16)$$

Since the transverse wavenumbers q_1, q_2, and $s_{44}^{(2)}$ are real and positive, therefore, to satisfy Eq. (16), the coefficient of elastic compliance $s_{44}^{(1)}$ must be negative, i.e. $s_{44}^{(1)} < 0$. Combining Eq. (16) and Eqs (10) and (11), we arrive at the following dispersion equation for the new elastic surface wave propagating along the interface between two semi-infinite half-spaces:

$$
\begin{aligned}
K(\omega) = \omega \cdot &\sqrt{\frac{s_{44}^{(2)} \cdot s_{44}^{(1)}(\omega)}{\left(s_{44}^{(2)} + s_{44}^{(1)}(\omega)\right)}} \\
&\cdot \sqrt{\frac{s_{44}^{(2)} \cdot \rho_1 - s_{44}^{(1)}(\omega) \cdot \rho_2}{\left(s_{44}^{(2)} - s_{44}^{(1)}(\omega)\right)}}, \quad (17)
\end{aligned}
$$

where the elastic compliance $s_{44}^{(1)}(\omega)$ in the metamaterial half-space is a function of angular frequency ω

and is given by $s_{44}^{(1)}(\omega t) = s_0 \cdot \left(1 - \omega_p^2/\omega^2\right)$ (see Eq. (1)). By contrast, the material constants $s_{44}^{(2)}$, ρ_1, and ρ_2 are frequency independent.

Dispersion Eq. (17) is an eigenvalue equation relating the wave number K with the angular frequency ω of the elastic surface wave. Equation (17) shows that for the wave propagation constant K to be positive, the elastic compliances of both half-spaces must meet the following condition:

$$\left(s_{44}^{(1)} < 0\right) \bigwedge \left(s_{44}^{(1)} + s_{44}^{(2)}\right) < 0. \qquad (18)$$

2.6. Phase velocity $v_p(\omega)$

The analytical formula for the phase velocity $v_p(\omega)$ of the new shear horizontal acoustic surface waves results immediately from Eq. (17), since $K = \omega/v_p$, i.e.:

$$v_p(\omega) = \sqrt{\frac{\left(s_{44}^{(2)} + s_{44}^{(1)}(\omega)\right)}{s_{44}^{(2)} \cdot s_{44}^{(1)}(\omega)}}$$
$$\cdot \sqrt{\frac{\left(s_{44}^{(2)} - s_{44}^{(1)}(\omega)\right)}{\left(s_{44}^{(2)} \cdot \rho_1 - s_{44}^{(1)}(\omega) \cdot \rho_2\right)}}. \qquad (19)$$

2.7. Group velocity $v_{gr}(\omega)$

The group velocity is defined as $v_g(\omega) = \mathrm{d}\omega/\mathrm{d}K$. Therefore, differentiating Eq. (17) with respect to ω, gives rise to the following analytical expression for the group velocity $v_g(\omega)$ of the new shear horizontal elastic surface wave:

$$v_{gr}(\omega) = \frac{1}{v_p(\omega)}$$
$$\cdot \frac{2 \cdot \left(\left(s_{44}^{(2)}\right)^2 - \left(s_{44}^{(1)}(\omega)\right)^2\right)}{2 s_{44}^{(2)} s_{44}^{(1)}(\omega)\left(s_{44}^{(2)} \cdot \rho_1 - s_{44}^{(1)}(\omega) \cdot \rho_2\right) + a^*}, \quad (20)$$

where

$$a^* = \omega s_{44}^{(2)} \frac{\mathrm{d} s_{44}^{(1)}(\omega)}{\mathrm{d}\omega}\left\{\left(s_{44}^{(2)} \cdot \rho_1 - 2 s_{44}^{(1)}(\omega) \cdot \rho_2\right)\right.$$
$$\left. + 2\left(s_{44}^{(1)}(\omega)\right)^2 \frac{\left(s_{44}^{(2)} \cdot \rho_1 - s_{44}^{(1)}(\omega) \cdot \rho_2\right)}{\left(s_{44}^{(2)}\right)^2 - \left(s_{44}^{(1)}(\omega)\right)^2}\right\},$$

$v_p(\omega)$ is the phase velocity given by Eq. (19), and

$$\frac{\mathrm{d} s_{44}^{(1)}(\omega)}{\mathrm{d}\omega} = +2 s_0 \frac{\omega_p^2}{\omega^3}.$$

Formula (20) allows for the plotting of the group velocity $v_{gr}(\omega)$ of the wave as a function of the circular frequency ω.

2.8. Power flow in the waveguide structure

The time averaged power density flux vector is represented by the complex acoustic Poynting vector **P** which has two components:

$$P_1(x_2) = -\frac{1}{2}\,\mathrm{Re}\left[\tau_{13}(-j\omega u_3)^*\right]$$

along the direction of propagation x_1, and

$$P_2 = -\frac{1}{2}\,\mathrm{Re}\left[\tau_{23}(-j\omega u_3)^*\right]$$

along the direction perpendicular to the interface (along the axis x_2) (Auld, 1990).

Employing Eqs (4), (5), (7), and (8) we get at the following formulas for the cycle-averaged components of the Poynting vector P_1 in the upper and lower half-spaces:

$$P_1^{\mathrm{lower}}(x_2) = \frac{1}{2}A^2 \frac{1}{s_{44}^{(1)}(\omega)} K(\omega) \cdot \omega \cdot \exp\left(2q_1 x_2\right), \quad (21)$$

$$P_1^{\mathrm{upper}}(x_2) = \frac{1}{2}B^2 \frac{1}{s_{44}^{(2)}} K(\omega) \cdot \omega \cdot \exp\left(-2q_2 x_2\right). \qquad (22)$$

From boundary condition (Eq. (12)), we can write $A = B$.

Analyzing formulas (21) and (22) we can notice that the power flow in the upper half-space P_1^{upper} is positive, while the power flow in the lower half-space P_1^{lower} is negative, thus vectors P_1^{upper} and P_1^{lower} are antiparallel. Moreover, Poynting vectors P_1^{upper} and $-P_1^{\mathrm{lower}}$ attain maximum at the interface ($x_2 = 0$) and diminish monotonically to zero with increasing distance from the interface.

The total power P_1^{total} carried by the surface wave in the propagation direction x_1 per unit width x_3 is obtained by integrating the power $P_1(x_2)$ in the upper and lower half-spaces along the coordinate x_2 perpendicular to the interface surface ($x_2 = 0$), namely:

$$P_1^{\mathrm{total}}(\omega) = \int_{-\infty}^{0} P_1^{\mathrm{lower}}(x_2)\,\mathrm{d}x_2 + \int_{0}^{+\infty} P_1^{\mathrm{upper}}(x_2)\,\mathrm{d}x_2$$
$$= \frac{1}{4}A^2 K(\omega) \cdot \omega \cdot \left(\frac{1}{s_{44}^{(1)}(\omega)}\frac{1}{q_1} + \frac{1}{s_{44}^{(2)}}\frac{1}{q_2}\right). \quad (23)$$

Since $s_{44}^{(1)}(\omega)$ and $s_{44}^{(2)}$ are of the opposite sign, therefore the overall power flow $P_1^{\mathrm{total}}(\omega)$ may, for a certain angular frequency ω, be cancelled out.

3. Results

3.1. Dispersion curve of the surface wave

The properties of the new acoustic elastic surface wave were analyzed on an exemplary waveguide

structure consisting of the metamaterial lower half-space ($x_2 \leq 0$) based on ST-Quartz with embedded local micro-resonators with a selected resonant frequency f_p = 1 MHz, and conventional PMMA elastic upper half-space ($x_2 \geq 0$). The material parameters of these two elastic semi-spaces are given in Table 1 (KIEŁCZYŃSKI, 2015). In our analysis, losses in the constituent half-spaces are neglected.

Table 1. Material parameters of two half-spaces of the waveguide: $s_0 = s_{44}^{(1)} (\omega \to \infty)$, see Eq. (1), phase velocity $v_0 = \sqrt{1/(s_0 \rho_1)}$.

Material	Density [kg/m³]	Elastic compliance [$\times 10^{-11}$ Pa^{-1}]	Bulk shear wave velocity [m/s]
ST-Quartz	ρ_1 = 2650	s_0 = 1.474	v_0 = 5060
PMMA	ρ_2 = 1180	$s_{44}^{(2)}$ = 70.03	v_2 = 1100

Using formula (17), the dispersion curve for the acoustic surface wave has been evaluated and plotted in Fig. 2. Here, the surface resonant frequency f_{sp} is equal to f_{sp} = 143.569 kHz.
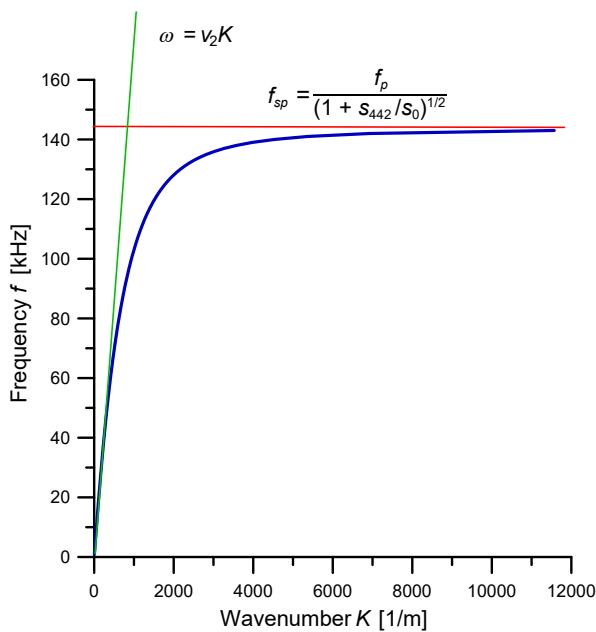

Fig. 2. Dispersion curve $\omega - K$ of new acoustic surface waves.

The dispersion curve ($\omega - K$) of the new SH elastic surface wave (Fig. 2), is in fact very similar to that encountered in SPP electromagnetic modes, propagating in metal-dielectric waveguides. The surface resonant frequency f_{sp} of the new elastic surface waves is approached asymptotically when the wavenumber $K \to \infty$. In this paper, the term "surface resonant frequency" corresponds to the term "surface plasma frequency", known in the theory of electromagnetic surface waves of the SPP type.

3.2. Phase velocity $v_p(\omega)$ of the surface wave

Phase velocity $v_p(\omega)$ of the acoustic surface wave was evaluated using formula (19). Plot of the phase velocity v_p as a function of frequency f is given in Fig. 3.
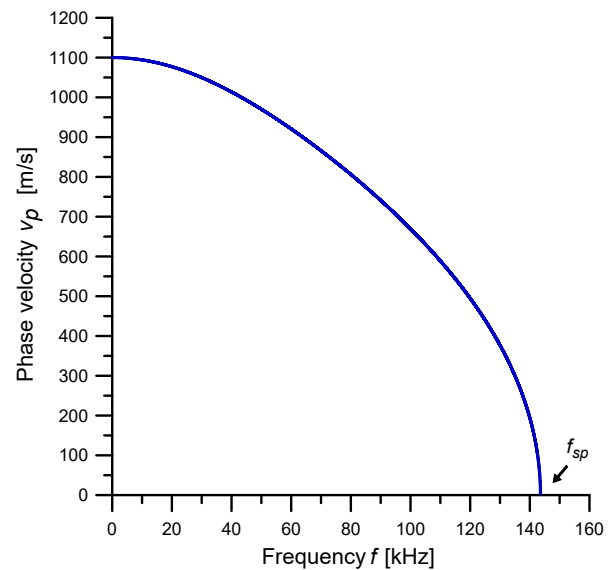

Fig. 3. Phase velocity v_p of the new surface wave versus frequency f. Note that, $v_p(\omega \to 0) \to v_2$ and $v_p(\omega \to \omega_{sp}) \to 0$.

3.3. Group velocity $v_{gr}(\omega)$ of the surface wave

The group velocity $v_{gr}(\omega)$ of the wave can be interpreted as the slope of the dispersion curve shown in Fig. 2.

Figure 4 shows dependency of the group velocity v_{gr} of the elastic surface wave as a function of fre-
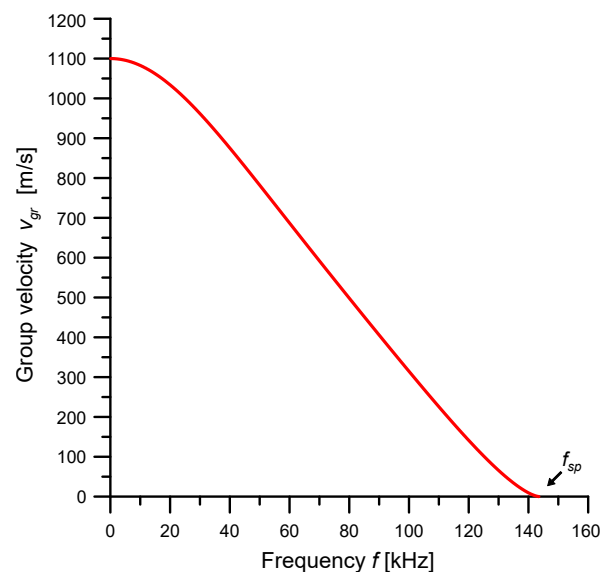

Fig. 4. Group velocity v_{gr} of the surface wave versus frequency f. Note that, $v_{gr}(\omega \to 0) \to v_2$ and $v_{gr}(\omega \to \omega_{sp}) \to 0$, similarly as phase velocity $v_p(\omega)$.

quency. The group velocity v_{gr} was evaluated according to the formula (20).

3.4. Mechanical displacement distribution

Employing the dispersion Eq. (17) and formulas (4, 7, 10, 11), the profile of the mechanical displacement $u_3(x_2)$ of the acoustic surface wave as a function of the distance $|x_2|$ from the interface is presented in Fig. 5.
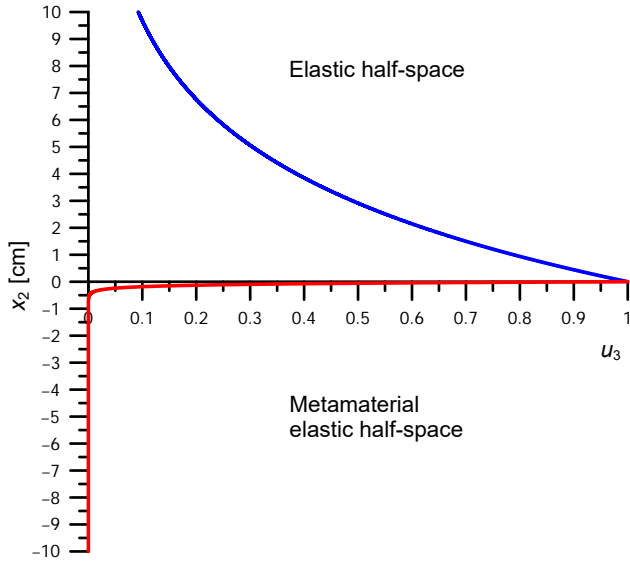

Fig. 5. Plot of the normalized mechanical displacement $u_3(x_2)$ versus the distance away from the interface ($x_2 = 0$) along the vertical axis x_2. Wave frequency $f = 20$ kHz, and $f/f_{sp} = 0.14$.

As can be seen in Fig. 5, the acoustic field u_3 of the surface wave in the direction perpendicular to the interface ($x_2 = 0$) is an evanescent field and decays monotonically to zero with $|x_2| \to \infty$. However, it is immediately apparent that the rate of the decay is considerable asymmetrical on both sides of the guiding surface. In fact, the mechanical displacement $u_3^{(1)}(x_2)$ in the elastic metamaterial $x_2 < 0$ approaches very quickly zero in contrast to the conventional elastic half-space $x_2 \geq 0$.

3.5. Power flow in the waveguide structure

The total power P_1^{total} carried by the surface wave in the propagation direction x_1 per unit width x_3 was plotted in Fig. 6 using formula (23). As can be seen in Fig. 6, the total power of the surface wave P_1^{total} tends to zero, when the wave frequency approaches the surface resonant frequency f_{sp}. This is a characteristic feature of this new acoustic surface wave. It should be noted that a similar property is also exhibited by electromagnetic surface waves of the SPP type (NKOMA *et al.*, 1974; ROSENBLATT *et al.*, 2010).

Since the new surface acoustic wave is an evanescent wave in the direction perpendicular to the inter-
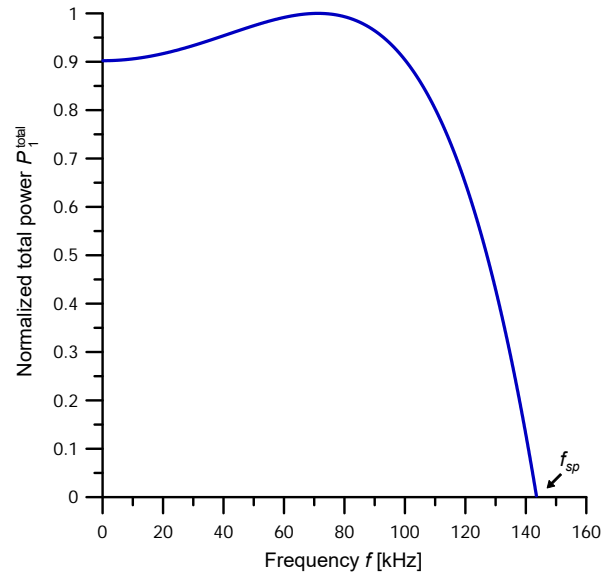

Fig. 6. Normalized total power P_1^{total} carried by the surface wave in the direction of propagation x_1, as a function of wave frequency f. Surface resonant frequency $f_{sp} = 143.569$ kHz.

face ($x_2 = 0$) along the x_2 axis, it can be proved that the total power of the surface wave P_2^{total} propagating in the direction of the x_2 axis is equal to zero.

4. Discussion

In this paper we analyze for the first time the properties of new SH acoustic surface waves that propagate at the interface between two elastic half-spaces, one of which is an elastic metamaterial with a very special elastic compliance $s_{44}^{(1)}(\omega)$, namely that is negative for $0 \leq \omega < \omega_p$ (Eq. (1)) in a perfect analogy to the dielectric function $\varepsilon(\omega)$ in Drude's model of metals (NKOMA *et al.*, 1974). To the best of our knowledge no such type of acoustic waves has been yet analyzed in the literature.

For low frequencies f, the phase v_p and group v_p velocities of the surface wave are approximately equal to v_2, i.e. the velocity of the transverse bulk waves in the elastic upper semi-space.

With increasing frequency (for $f \to f_{sp}$), where f_{sp} is the surface resonant frequency:

$$f_{sp} = \frac{f_p}{\sqrt{1 + s_{44}^{(2)}/s_0}},$$

the phase velocity v_p and group velocity v_{gr} of the elastic surface wave decrease monotonically to zero.

An interesting feature of the proposed surface acoustic wave is that the power of the surface wave in the upper half-space propagates in opposite direction than the power in the lower half-space. Consequently, the total power P_1^{total} carried by the surface

wave in the direction of propagation x_1 converges to zero, as the wave frequency approaches the surface resonant frequency f_{sp} (Fig. 6).

As can be seen in Figs 2, 3, and 4, the phase v_p and group v_{gr} velocities of a new surface acoustic wave are always inferior to the velocity v_2 of bulk shear waves in the upper half-space.

Moreover, the group velocity of the wave (Fig. 4) is always lower than the phase velocity (Fig. 3), for all frequencies less than the surface resonant frequency, i.e. for $f < f_{sp}$.

As shown in Fig. 5, the acoustic field is spatially confined to the interface $x_2 = 0$. The mechanical displacement u_3 of the surface wave reaches its maximum at the interface, and decreases exponentially in both elastic half-spaces as the distance from the interface increases for $|x_2| \rightarrow \infty$.

For higher frequencies ($f \rightarrow f_{sp}$) the penetration depth of the mechanical displacement u_3 of the surface wave into the upper and lower semi-spaces, is approximately the same. In this case the penetration depth can be even lower than the wavelength, for example: for a frequency equal to 143 kHz, that is, for $f/f_{sp} = 0.995$, the penetration depth into the upper half-space $\delta_{\text{upper}} = 1/q_2$ is equal to 87 μm and the penetration depth into the lower half-space $\delta_{\text{lower}} = 1/q_1$ equals 86 μm. It should be noted that the wavelength in this case is equal to 540 μm, i.e. the penetration depth is over six times smaller than the wavelength.

At lower frequencies ($f \rightarrow 0$), the penetration depth into the upper half-space is much larger than that into the lower half-space, for example: for $f = 10$ kHz, i.e. for $f/f_{sp} = 0.07$, the penetration depth into the lower metamaterial elastic half-space δ_{lower} equals 0.8 mm, while the penetration depth into the upper elastic half-space δ_{upper} equals 169.3 mm Here, the wavelength equals 109.4 mm. And similarly, at $f = 20$ kHz, i.e. for $f/f_{sp} = 0.14$, the penetration depth into the lower metamaterial elastic half-space δ_{lower} equals 0.8 mm, while the penetration depth into the upper elastic half-space δ_{upper} equals 42 mm. Here, the wavelength equals 53.7 mm.

The phase v_p and group velocity v_{gr} of the new surface wave slow down when the wave frequency f

Table 2. Phase v_p and group velocity v_{gr}, penetration depths in the upper δ_{upper} and lower δ_{lower} half-spaces and wavelength λ for various wave frequencies f.

f [kHz]	v_p [m/s]	v_{gr} [m/s]	δ_{upper} [mm]	δ_{lower} [mm]	λ [mm]
10	1094.2	1082.7	169.3	0.805	109.4
20	1077.1	1034.0	42.2	0.802	53.7
50	970.2	782.2	6.55	0.780	19.4
140	194.2	9.45	0.224	0.213	1.39
143	77.6	0.61	0.087	0.086	0.54

approaches the surface resonant frequency f_{sp} (Figs 3 and 4). For example at a frequency $f = 140$ kHz, $v_p = 194.2$ m/s and $v_{gr} = 9.5$ m/s and subsequently at a frequency $f = 143$ kHz, $v_p = 77.6$ m/s and $v_{gr} = 0.61$ m/s, respectively. Here, the surface resonant frequency $f_{sp} = 143.569$ kHz. The above results can be summarized in Table 2.

5. Conclusions

From the results of the research presented in this study, the following main conclusions can be drawn:

1) We have demonstrated that a pure SH acoustic surface wave can propagate along the plane interface between two rigidly bonded elastic semi-spaces, where one of the semi-infinite medium is an elastic metamaterial with negative elastic compliance. It is worth noting that according to the classical elastic wave theory, the shear horizontal surface acoustic waves cannot occur at the interface between two pure elastic semi-spaces.

2) In the low frequency range (wavenumbers), the new surface acoustic wave has a large penetration depth of the acoustic field into the upper conventional elastic half-space. Whereas the penetration depth into the lower (metamaterial) semi-space is small.

3) In the frequency range close to the surface resonant frequency f_{sp} (for large wavenumbers K), the energy of the surface acoustic wave is concentrated in the proximity of the interface ($x_2 = 0$). The acoustic field of the surface wave penetrates into the upper and lower half-spaces at a distance shorter than the wavelength.

4) The phase v_p and group v_{gr} velocities of the new acoustic wave slow down and tend to zero as the wave frequency f approaches the surface resonant frequency f_{sp}. This property can result in an exceptionally large sensitivity of the new wave to mass loading on the interface.

5) The Poynting vectors of the new SH acoustic surface wave in the upper half-space P_1^{upper} and lower half space P_1^{lower} are always oriented in opposite directions along the axis x_1. The total power $P_1^{\text{total}} = P_1^{\text{lower}} + P_1^{\text{lower}}$ carried by the surface wave in the direction of propagation x_1 converges to zero, when the wave frequency tends to f_{sp}.

6) This new SH acoustic surface wave exhibits some similarities to the shear horizontal Maerfeld–Tournois acoustic wave which propagates at the interface of two elastic half spaces, at least one of which is a piezoelectric body. In both types of waves, the mechanical displacement of the wave decays monotonically to zero with increasing distance from the interface ($x_2 = 0$).

7) The mathematical model describing the new surface acoustic wave is very similar to the mathematical model describing electromagnetic surface waves of the SPP type. Therefore, this new acoustic surface wave inherits much of the properties of SPP electromagnetic waves and can be considered as an elastic (acoustic) analog of an electromagnetic surface wave of the SPP type.

The penetration depth of the new acoustic wave can be smaller than the wavelength λ (e.g. of the order of $\lambda/10$). Due to this strong concentration of the acoustic field in the vicinity of the interface, the proposed new SH surface acoustic wave can be applied in extremely highly sensitive sensors of physical quantities (e.g. viscosity), biosensors, chemosensors, near field acoustic microscopy (with subwavelength resolution), as well as in miniaturized micro and nano-scale modern acoustic devices.

Acknowledgments

References

1. ACHENBACH J.D. (1973), *Wave Propagation in Elastic Solids*, North-Holland, Amsterdam.

2. AMBATI M., FANG N., SUN C., ZHANG X. (2007), Surface resonant states and superlensing in acoustic metamaterials, *Physical Review B*, **75**(19): 195447, doi: 10.1103/PhysRevB.75.195447.

3. AULD B.A. (1990), *Acoustic Fields and Waves in Solids*, Vol. I, II, Krieger Publishing Company, Florida.

4. BLEUSTEIN J.L. (1968), A new surface wave in piezoelectric materials, *Applied Physics Letters*, **13:** 412-413, doi: 10.1063/1.1652495.

5. BORN M., WOLF E. (1980), *Principles of Optic,* 6th ed., p. 625, Cambridge University Press, Cambridge.

6. DENG K., HE Z., DING Y., ZHAO H., LIU Z. (2014), Surface-plasmon-polariton (SPP)-like acoustic surface waves on elastic metamaterials, *arXiv*, doi: 10.48550/arXiv.1408.2186.

7. KADIC M., BÜCKMANN T., SCHITTNY R., WEGENER M. (2013), Metamaterials beyond electromagnetism, *Reports on Progress in Physics*, **76**(12): 126501, doi: 10.1088/0034-4885/76/12/126501.

8. KIEŁCZYŃSKI P., SZALEWSKI M., BALCERZAK A., WIEJA K. (2015), Group and phase velocity of love waves propagating in elastic functionally graded materials, *Archives of Acoustics*, **40**(2): 273–281, doi: 10.1515/aoa-2015-0030.

9. KIEŁCZYŃSKI P. (2018), Direct Sturm–Liouville problem for surface Love waves propagating in layered viscoelastic waveguides, *Applied Mathematical Modelling*, **53**: 419–432, doi: 10.1016/j.apm.2017.09.013.

10. KIEŁCZYŃSKI P. (2021), *New Fascinating Properties and Potential Applications of Love Surface Waves*, Invited Speaker presentation at the IEEE, International Ultrasonic Symposium, September 11–16, 2021, Xi'an, China, http://zbae.ippt.pan.pl/strony/publikacje.htm.

11. LOVE A.E.H. (1911), *Some Problems of Geodynamics*, Cambridge University Press, London.

12. MAERFELD C., TOURNOIS P. (1971), Pure shear elastic surface wave guided by the interface of two semi-infinite media, *Applied Physics Letters*, **19**(4): 117, doi: 10.1063/1.1653836.

13. MAIER S.A. (2007), *Plasmonics: Fundamentals and Applications*, Springer, Berlin.

14. NKOMA J., LOUDON R., TILLEY D.R. (1974), Elementary properties of surface polaritons, *Journal of Physics C: Solid State Physics*, **7**(19): 3547–3559.

15. ROSENBLATT G., FEIGENBAUM E., ORENSTEIN M. (2010), Circular motion of electromagnetic power shaping the dispersion of surface plasmon polaritons, *Optics Express*, **18**(25): 25861–25872, doi: 10.1364/OE.18.025861.

16. ROYER D., DIEULESAINT E. (2000), *Elastic Waves in Solids I*, Springer, Berlin Heidelberg New York.

17. WU Y., LAI Y., ZHANG Z.-Q. (2011), Elastic metamaterials with simultaneously negative effective shear modulus and mass density, *Physical Review Letters*, **107**(10): 105506, doi: 10.1103/PhysRevLett.107.105506.

18. YU S.-Y. *et al.* (2020), Slow surface acoustic waves via lattice optimization of a phononic crystal on a chip, *Physical Review Applied*, **14**(6): 064008, doi: 10.1103/PhysRevApplied.14.064008.

19. ZACCHERINI R. *et al.* (2020), Locally resonant metasurfaces for shear waves in granular media, *Physical Review Applied*, **13**(3): 034055, doi: 10.1103/PhysRevApplied.13.034055.

20. ZHANG J., ZHANG L., XU W. (2020), Surface plasmon polaritons: physics and applications, *Journal of Physics D: Applied Physics*, **45**(11): 113001.